CONF-9110289--3

DE92 007835

WORLD SCIENTIFIC PUBLISHING CO. PTE. LTD.

LASER SPECTROSCOPY AND LASER ION SOURCE DEVELOPMENT AT UNISOR

CARROL BINGHAM

Department of Physics and Astronomy, University of Tennessee
Knoxville, TN 37996-1200, USA

ABSTRACT

The development of the laser spectroscopy facility at UNISOR will be described. The method of collinear laser-atomic beams interaction is utilised to achieve atomic spectra essentially free of Doppler spreading. Measurement of resonance fluorescence via an efficient fiber-optic light collector is used to observe the atomic excitation by the laser beam. The system has been utilised to measure the atomic lifetime of the $6p^1P_5/2^0$ level in Xe II. In another experiment the relativistic Doppler effect was measured as a test of time dilation. Hyperfine structure and isotope shift measurements have been made for a series of Tl atoms ranging in mass from 187 to 205. Magnetic dipole and electric quadrupole moments were deduced for several of these isotopes; these quantities and the isotope shifts added greatly to our understanding of nuclear shapes in this transition region. Future directions will focus around more sensitive detection techniques and the development of purer beams in order to enable the study of nuclei farther from stability. The development of a laser ion source which operates in a completely cold mode and utilises resonant absorption in the ionisation process would facilitate the production of ultra-pure atomic beams.

1. Introduction and Method

1.1. Value of Laser Spectroscopy in the Study of Nuclei

There are several fundamental properties of a nucleus that provide rigid tests of nuclear structure theory and nuclear models. These are the energy levels, the spins and parities of these levels, and the nuclear matter distribution. Much of our information about nuclei comes from the study of transitions between nuclear levels, transitions that are characteristic of the changes in quantum numbers but generally not dependent on the absolute value of a quantum number of either the initial or final state. Thus, methods to determine the spins and nuclear moments and sizes of nuclear ground states are crucial to measurement and understanding of nuclear structure. One method to determine properties of the nuclear ground state is to measure properties of atomic spectra which depend on the nuclear properties. The hyperfine structure (hfs) seen in atomic transitions is a direct consequence of the atomic electrons interacting with the various moments of the nuclear charge distribution and hence provides a means to measure these moments. In odd-A nuclei the magnetic moment is crucially dependent on the orbit of the odd nucleon and hence provides a valuable clue to the structure of the state. The quadrupole moment

is an indicator of how much the nuclear charge distribution deviates from spherical shape. Also, the spacings between atomic energy levels are dependent on the size of the charge distribution, even in those cases where only the monopole moment acts, and shifts in nuclear size from isotope to isotope can be traced as a shift in frequency of atomic transitions. Thus, optical spectroscopy can provide sensitive measurements of the properties of nuclear ground states and isomers. These in turn provide a tie point for gamma and conversion electron spectroscopy to determine the crucial quantum numbers for the excited states.

1.2. Doppler Free Spectroscopy at UNISOR

In 1970 Otten[1] pointed out that the then recently developed tunable dye lasers should enable a high sensitivity for hfs measurements thus enabling the use of optical spectroscopy to study exotic nuclides. Subsequently, Duke, et al.[2] used a dye laser to determine $\delta < r^2 >$ for ^{190}Hg, and very significantly, they showed that the measurements could be made with less than 10^{10} atoms. In 1976 Kaufman[3] proposed a technique utilizing collinear beams of fast atoms or ions and laser light. This technique had two very important advantages over doing the optical spectroscopy in a cell: 1)the line width due to the Doppler broadening can be reduced significantly (reduction of 1/1000 for heavy atoms at 50 keV), and 2) the sensitivity is improved. Soon thereafter this technique was shown to be feasible in two demonstration experiments.[4,5] Early in 1978 the UNISOR collaboration decided to investigate the feasibility of on-line laser spectroscopy measurements of nuclear spins, magnetic moments, quadrupole moments, and isotope shifts. Over the course of two or three years, a collinear laser-ion beam facility was designed, a proposal to obtain capital funds was written and approved, considerable reconfiguration of the UNISOR facility was carried out and the new laser-ion beam line built, and the laser equipment was partially purchased and partially built. The first published description of the system being built at UNISOR appeared in 1980,[6] and over the years a total of 13 publications and numerous talks have been presented concerning the facility and the measurements made. In recent years the beam line has been restructured and modifications have been made in the measurement techniques. In this review paper, systems will be described and several measurements will be discussed. Possible future directions will be discussed briefly.

2. UNISOR Laser Spectroscopy Facility

The layout of the parallel laser-ion beam facility[7] is shown in Fig. 1a. The laser beam prepared outside the vacuum chamber enters the chamber through a Brewster window and merges with the ion beam between the plates of an electrostatic deflector. The two beams then pass through entrance and exit collimators to assure collinearity. For experiments requiring spectroscopy on the neutral atom, the ion beam passes into a charge exchange cell where neutralization occurs with an efficiency that depends on the atomic species. Following the charge exchange cell is the interaction region. For most of the experiments carried out at UNISOR, an ion

collected simultaneously from a calibration standard. The standard which we used was I_2. The I_2 spectrum is comprised of multiplets which are well-understood and whose centroids have been measured and catalogued.[8] Through the use of saturation spectroscopy, these multiplets were resolved and the individual components used to get more precise calibration. In addition a portion of the laser light was sent to a 150-MHz etalon which generated a spectrum with peaks separated by this constant amount, thus providing a scale to determine frequency differences in the spectra.

Although the I_2 calibration spectrum has the potential of giving the absolute wavelength, the complicity of the spectrum makes it difficult to discover what part of the spectrum is being observed. Thus, we found it useful to build a wavemeter to give us a rather precise measure of the wavelength in order to find the correct part of the spectrum to use and to aid in setting the scan range for a spectroscopy experiment.[9] The wavemeter incorporates a division-of-amplitude type of interferometer which is used to produce two sets of fringes, one due to the unknown laser wavelength and another from a reference laser whose wavelength is accurately known. In our wavemeter a Lamb-dip stabilized HeNe laser was used for the reference. As one of the mirrors of the interferometer is moved through some distance, the number of fringes from the two sources are counted simultaneously. The unknown wavelength is then given by the relationship

$$\lambda_u = \lambda_R \ N_R/N_u \tag{1}$$

where λ_R is the reference wavelength and N_u, N_R are the number of fringes from the unknown and reference beams. The accuracy of the measurement depends on the precision with which the number of fringes are measured and for either beam, a fraction of a fringe up to 1 might be missed due to the fact that the total distance moved is not an integral number of wavelengths. In order to make the distance the mirror moves during the measurement equal to an integral number of wavelengths for both the reference and unknown beams, a coincidence circuit was incorporated to start and stop the counts when the two fringes were observed to be in coincidence. With this technique the precision of the instrument was improved by a factor of ~ 15 over what could be achieved by using random starts and stops for the counting. Thus, the wavemeter achieved a precision of $5/10^7$ which is adequate to locate the correct range to establish a 30 GHz scan to pickup any known resonance transition.

Another way to scan the frequency seen by the particle beam is to lock the laser frequency and vary the velocity of the particles. Because of the Doppler effect, variation of the particle speed is equivalent to variation of the frequency of the laser light that is interacting. During the last few years we have modified the laser-ion beam line by adding several diagnostic tools, making the line modular to enable relatively easy changes in the beam line, and adoption of Doppler scanning rather than laser scanning. The beam line configuration[10] most recently used is shown in Fig. 1b. This experiment which was the study of the hyperfine structure of $^{187-185}$Tl utilized a Na charge exchange cell to neutralize the Tl ion beam. The velocity of the neutral Tl atoms was varied continuously by scanning the voltage applied to the charge exchange cell over a range from -500 to +500 V. In addition,

the entire scanning power supply could be raise[illegible] of 3000 V in order to accomodate rather large shifts in the scanning regi[illegible]ddition of a quadrupole lens and other beam optic elements aided in getting a go[illegible]ransmission through the interaction region, as did the use of a channelplate detector that could be inserted into the particle beam to monitor weak currents.

3. Atomic Lifetime Measurements

A technique was developed to use the collinear laser-ion beam setup to measure the lifetimes of excited ionic states of atoms.[11] The lifetime of an excited state is measured by observing the distance that the ions travel while moving at a given velocity before they emit a photon to return to a lower state. The ions are excited into the state of interest by interaction with the laser beam in the production zone and the excited state is observed to decay in the observation zone. By variation of the distance between the production zone and the observation zone, one can determine the decay rate with distance and convert this into the decay rate with time, which follows an exponentially decreasing curve, the slope of which determines the lifetime of the state.

The technique used to vary the distance between the production zone and the observation zone is illustrated in Fig. 2 (parts a-c). Both of these regions are contained within a parallel plate capacitor with cylindrical geometry and coaxially aligned with the beams. A potential applied accross the plates uniformly accelerates or decelerates the ion beam as it passes along the axis between the plates. The detection zone was fixed by use of a 30 cm Czerny-Turner spectrometer placed at right angles to the laser and ion beams. Two 20 cm focal length lenses were used to image the vertical entrance slit of the spectrometer in a 1:1 ratio onto the beam path. A sampling of the photons emitted by the excited ions in this limited zone were detected in the spectrometer by means of a cooled photomultiplier and single photon counting electronics. The position of the production zone was dependent on the frequency of the laser, since because of the Doppler effect a different frequency is required to be in resonance with the ions at each different velocity along the path between the capacitor plates. Thus, by scanning the laser frequency, one is in effect scanning the distance between the production zone and the detection zone.

The signals from the single photon counting electronics were used to generate a spectrum of the number of de-excitations observed as a function of frequency. Due to the correlation of the frequency with the position of production the spectrum displays the time dependence of the count rate. As shown in Ref. 11 the transformation from frequency intervals to time intervals is linear to first order, the proportionality constant depending only on the mass and charge of the ion, the resonant wavelength, and the electric field E. Since the count rate would fall exponentially with time, the spectrum should display a simple exponential fall-off. The electric field E was made quite constant by use of six different plates and a precision resistor chain to distribute the change in potential through the region. The linearity was checked by applying accurately measured voltages to both field

or atom was excited from the initial state to an excited intermediate state which then radiated a photon to a final state. The detection of the radiated photon was the signal used to ascertain that a laser photon was indeed resonantly absorbed. Since the beams are parallel throughout the charge-exchange cell and interaction region and any space between the two, it is possible for the beams to interact before they reach the detection region. This is not a problem if the initial and final states are the same state, but often they are not and the resulting optical pumping destroys any chance of observing the resonant absorption of the beam. One way that we have eliminated this problem is to superimpose a magnetic field on the region around the charge exchange cell to Zeeman shift the lines away from the resonant frequency until the atoms reach the detection region.

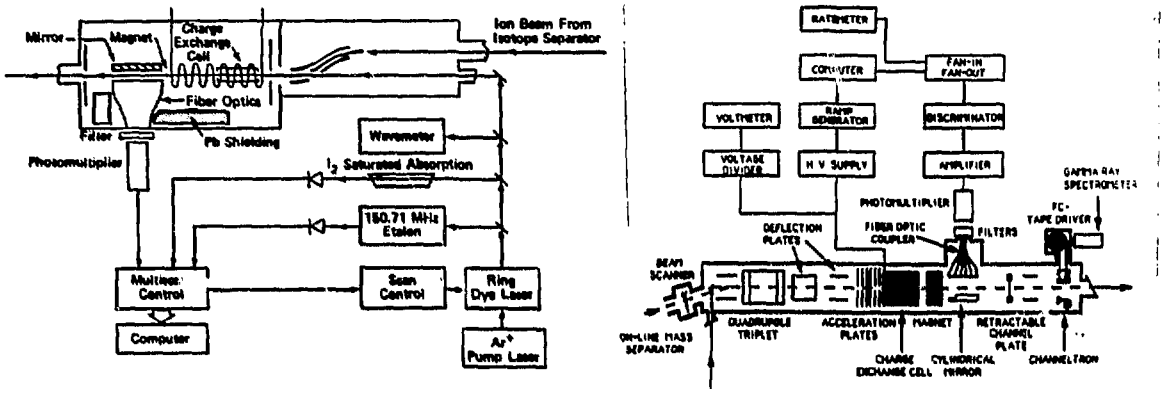

Figure 1. (a)Schematic of the UNISOR laser facility when configured to scan the laser frequency to observe resonances. (b) Schematic of the interaction region for the experiments where Doppler tuning was used to observe resonances.

Various light detectors have been used for various experiments carried out at UNISOR and these will be discussed for three of these in the sections to follow. Following the interaction-detection region the ions and/or atoms are stopped. To measure transmission efficiencies and to tune the beam through the apparatus, a faraday cup and a channeltron were often used.

In order to observe an unknown absorption resonance, a measurement over a range of frequencies is required. Thus, one must scan the frequency seen by the interacting beam through a region of possible interest and measure the interaction rate at each frequency. The setup shown in Fig. 1a includes a scanning dye laser which is pumped with an Argon laser. Nearly 1 watt of laser power can be extracted from the scanning dye laser. The frequency can be scanned over a range of 30 GHz or any smaller range. The scan controller generates a voltage signal which is proportional to the current frequency minus the base frequency of the range being scanned. Thus, by feeding this voltage to an ADC gated by photons detected from the interaction region, one can display the absorption spectrum as a histogram. This method has the advantage of direct comparison of the spectrum with another

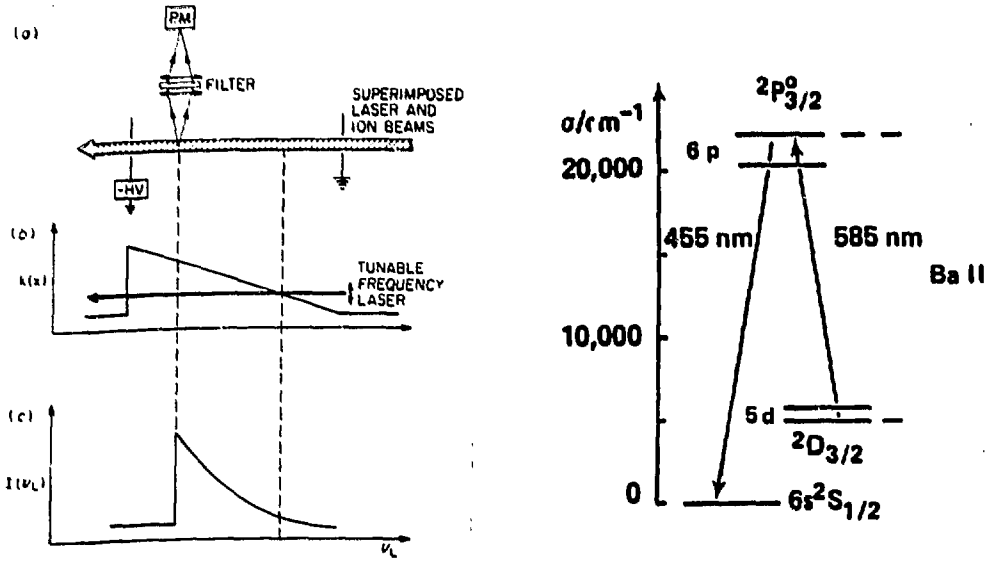

Figure 2. Principle of the rapid Doppler switching method. (a) Schematic of the experimental arrangement showing the collinear beams passing through a parallel plate capacitor. (b) The ion kinetic energy as a function of position along the common beam axis. (c) The expected variation of the recorded fluorescence as a function of laser frequency. (d) Partial energy level diagram of Ba II showing the transitions used in the present investigation.

plates of the capacitor and observing the shift of the spectrum.

The feasibility of this method was tested by measurement of the well-known[12] lifetime of the $6p^2P^o_{3/2}$ level in Ba II. As shown schematically in Fig. 2d, Ba ions in the $^2D_{3/2}$ metastable state present in the beam from the isotope separator were excited via a 585 nm laser radiation to the state of interest. The Czerny-Turner spectrometer was used to detect the 455 nm photons emitted by these excited ions in the detection region. The laser was scanned over a 10 GHz region encompassing the 585 nm absorption line suitably shifted to account for the Doppler shift. A series of rapid scans were made in order to avoid the necessity to correct the spectra for fluctuations in ion- or laser-beam intensities. The fluorescence from the $6p^2P^o_{3/2}$ level and from the I_2 cell were used to trigger two ADCs which stored the frequency shift of the laser at the time of each detected event. The I_2 spectrum was taken to check for mode hops and to monitor small drifts over long periods of time. Frequency markers from a 1.5 GHz etalon were also used in calibrating the spectra.

A set of the Ba II $6p^2P^o_{3/2}$ decay data and the accompanying I_2 spectrum is shown in the left part of Fig. 3. A dead time correction (always <1%) was applied to the data in each channel independently using standard techniques. The fluorescence shows a buildup and decay character. The region of the peak results from excitation in the detection zone and the high channel part of the spectrum corresponds to

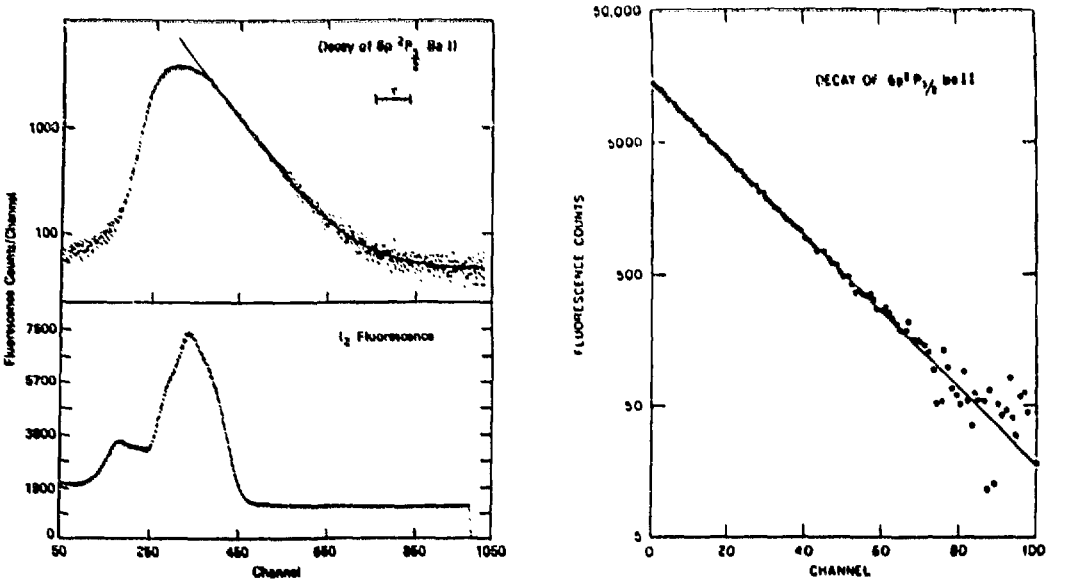

Figure 3. (a) Decay of the fluorescence at 455 nm in Ba II. While the influence of the instrumental window function is obvious at channels near the peak, its effect becomes negligible at larger channels as shown by the solid curve which is composed of a single exponential plus a constant. (b) The I_2 vapor reference spectrum used in these measurements to monitor laser frequency changes. (c) A semilogarithmic plot of the Ba decay data with the constant background subtracted, and the least-squares fit with a single exponential function.

having the production zone well separated from the detection zone. Outside the window region the total spectrum can be interpreted as being a superposition of peaks that resulted from production at various production zones along the beam path, with each successive peak being reduced by the decay. Away from the window region the slope of the resulting curve just reflects the lifetime of the state that is fluorescing. This hypothesis was tested by fitting the data above the peak with a function of the form $N = N_o exp(-t/\tau) + B$, where N_o, B and τ are constants determined by the method of least squares. For starting channels well above the peak position, the result was independent of the actual starting channel, which shows that this region does follow an exponential plus a small constant background very well. This is demonstrated by comparing the exponentially decreasing curve with the data after the small background was subtracted in Fig. 3c.

Several independent measurements were made and the results of each measurement agreed well with each other. The unweighted average of the results is 6.35±0.05 ns which agrees with the accurate measurement by Andrã[12] of 6.312±0.016 ns. A careful analysis of the systematic errors associated with beam alignments, intensity variation with frequency, the finite lengths of the production and detection zones, and state mixing by an electric field was reported in Ref. 11. Including

systematic errors, an error of 0.09 ns was quoted.

This new technique was then used[13] to measure the lifetime of the $6p^4P^o_{5/2}$ level in Xe II. In this case the level under study was selectively excited from the $5d^4D_{7/2}$ metastable level which was produced with sufficient intensity in the separator ion source. The resonant absorption of the laser light by the moving ions was monitored by the fluorescence at 529.2 nm which is emitted in the radiative decay of the $6p^4P^o_{5/2}$ to the $6s^4P_{5/2}$ level. Again the data were well fit by a single exponential and a small constant background. Table 1 shows the result of the UNISOR work in comparison with previous measurements of this lifetime as well as one more recent measurement. Our value is the average of 10 independent measurements, which showed a statistical error of less than 1%. We have included our estimate of the systematic error in the value shown in the table. It is noted that our value is somewhat larger than the two previous measurements of comparable precision.[16,17] Although we did not know the origin of the differences,[13] it is gratifying to note that a more recent measurement,[18] also utilizing the crossed-beam technique gives a result that agrees with our result.

Table 1. Lifetime measurements on the $6p^4P^o_{5/2}$ level in Xe II.

Method	Result (ns)	Reference
Beam-foil spectroscopy	10.5±1.0	14
Electron beam - delayed coincidence	11.5±1.5	15
Photon-photon delayed coincidence	7.47±0.27	16
Crossed laser-ion beams	7.53±0.15	17
Parallel laser-ion beams	7.95±0.16	13 (UNISOR)
Crossed laser-ion beams	7.90±0.15	18

4. A Test of Special Relativity

According to classical mechanics the interaction frequency of a wave with a particle in parallel motion with the wave is given by the formula

$$\nu = \nu_o/(1 \pm \beta) \tag{2}$$

where β = u/c, u is the speed of the particle, and ν_o is the interaction frequency when the particle is at rest in the medium of the wave. A relativistically correct result must include the time dilation factor and results in the formula

$$\nu = \nu_o \frac{(1-\beta^2)^{1/2}}{1 \pm \beta}. \tag{3}$$

In both formulas the + or - signs result when the wave and particle motions are parallel or antiparallel in the laboratory. If we adopt the notation of $\nu_+ = c\sigma_+$ for parallel beams and $\nu_- = c\sigma_-$ for antiparallel beams, and assume the particle will have equal speeds for both parallel and antiparallel measurements, we can easily show that the three wavenumbers are related as follows:

$$\sigma_o = \sqrt{\sigma_+ \sigma_-} \tag{4}$$

for the relativistically correct case, and

$$\sigma_o = \frac{2\sigma_+\sigma_-}{\sigma_+ + \sigma_-} \tag{5}$$

for the nonrelativistic calculation. These resulting equations only depend on the three measurable wave numbers and hence provide a means to test the time dilation factor used in special relativity.

By measuring the wavenumbers with both parallel beams (σ_+) and with antiparallel beams (σ_-), the wavenumber in the rest frame can be deduced with either the classical or the relativistically correct formulas above. The result can be compared with the wavenumber measured in the rest frame to test the respective formulas. An advantage of this technique is that the velocity of the interacting particles does not have to be known, and thus very accurate frequency measurements suffice to test the theory.

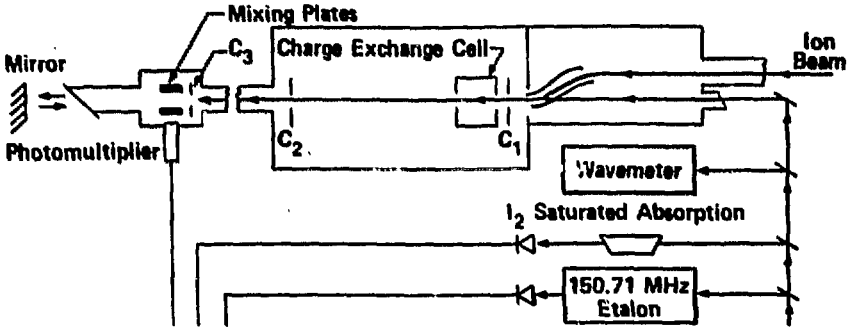

Figure 4. Schematic of the interaction region of the UNISOR laser facility when configured to measure resonating wavenumbers for parallel or antiparallel beams.

The experimental arrangement for these measurements[19] is shown in Fig. 1a, but with the interaction region modified as shown in Fig. 4. Hydrogen was chosen for the atomic beam since the H_α D1 wave number has been accurately measured,[20] and its small mass allows one to achieve the highest beam velocity with the acceleration voltage of the isotope separator, which was used to prepare the hydrogen ion beam. The resonance detection scheme was similar to that of Arnold *et al.*[21] The 50 keV H^+ beam passes through the Cs charge-exchange cell which places about 10% of the H^+ beam in the 2S and 2P states of H. The 2P states decay to the ground state rapidly, while the 2S states survive until the atoms reach the mixing plates. A small electric field applied to the plates causes the 2S and 2P levels to mix, resulting in the emission of Lyman α photons which are detected by the photomultiplier. When a laser beam with the correct frequency to elevate the atoms in the 2S level to the 3P level is superimposed on the atom beam, a strong depopulation of the 2S states occurs before the atoms reach the detection region, thus resulting in a decrease in the number of Lyman α photons detected. Consequently, as the laser is scanned over the resonance region, the Ly_α count rate

will go through a dip. The absolute frequencies at the resonances was determined by simultaneously observing the spectrum of I_2 with saturated absorption spectroscopy. Finally, the scale of the spectra was accurately determined by use of a 150.71 MHz etalon.

Several runs were carried out; typical experimentally determined values are $\sigma_+ = 15394.6640$ and $\sigma_- = 15073.5334$ cm^{-1}. Using both the classical and relativistic formulas discussed above, eight independent measurements for the D1 wavenumber were obtained. The averages of these are $\sigma_{o,r} = 15233.2549 \pm 00.10$ cm^{-1} and $\sigma_{o,c} = 15232.4093 \pm 0.0010$ cm^{-1}. The error given here is the variance calculated from the individual measurements. The accepted value[21] is $\sigma_o = 15233.25673 \pm 0.00005$ cm^{-1}.

For the experiment carried out at UNISOR the magnitude of the wavenumber shift due to time dilation is just given by $\sigma_{o,r} - \sigma_{o,c} = 0.8456$ cm^{-1}. From a thorough analysis of the sources of error[19] we estimated that our errors would be due to misalignment (0.0002 cm^{-1}), voltage drift (0.0011 cm^{-1}), position of individual I_2 peaks (0.0032 cm^{-1}), and H centroid (0.0025 cm^{-1}). Adding these in quadrature gives a total experimental error of (0.0042 cm^{-1}). It is clear that the value we obtained for $\sigma_{o,r}$ agrees with the accepted value of σ_o to within this estimated error. The accuracy of the time dilation correction is checked to an accuracy or $5/10^3$ by these measurements. It was projected in Ref. 19 that the accuracy could be improved by a factor of 10 by use of a two laser-atom beam setup and accurate measurement of the individual components of the hfs multiplets in the I_2 spectrum.

5. Nuclear Structure of Light Thallium Isotopes

The most extensive study to date utilizing laser spectroscopy at UNISOR has been the measurement of the hfs and isotope shifts of a number of Tl isotopes, ranging in mass from 205 down to 187. The setup shown in Fig. 1a was used for measurements down to mass 189,[22,23] and the setup of Fig. 1b was used for extension of the measurements to mass 187.[10] The very neutron deficient isotopes $^{187-194}$Tl were produced by the bombardment of Ta foils with ^{16}O projectiles from the Holifield Heavy-Ion Research Facility tandem accelerator. After ionization in the UNISOR ion source the separated isotope beams were directed into the laser spectroscopy regions shown in Fig. 1. By passing through a charge exchange cell containing Na vapor, the Tl ion beam was very efficiently transformed into a beam of atoms in the metastable 6p $^2P_{3/2}$ state. By use of a laser beam with a wavelength of about 535 nm, these metastable atoms can be excited to the 7s $^2S_{1/2}$ state which quickly decays via emission of a 377 nm photon to reach the ground state. The 377 nm photons from 11 cm of the beam path were collected with a fiber optics system and cylindrical mirror and routed to a cooled photomultiplier. Optical filters were used between the fiber optic collector and the photomultiplier to reduce background from scattered laser light. The photomultiplier signals were used as discussed in sec. 2 above to observe the hyperfine structure of the 6p $^2P_{3/2}$ and 7s $^2S_{1/2}$ states and the isotope shifts in the 535 nm transition in the Tl isotopes studied.

The spectrum from ^{193}Tl, shown in Fig. 5, is one of the richer ones; it contains three peaks resulting from a portion of the Tl beam with its nucleus in the $1/2^+$ ground state and six peaks resulting from the part of the beam with the nucleus in the $9/2^-$ isomeric state. The hfs associated with the atoms having the nucleus in the ground state was used to deduce the magnetic moment of the ground state using standard techniques outlined in Ref. 23. The hfs associated with the nuclear $9/2^-$ states was used to deduce both magnetic and spectroscopic quadrupole moments for these nuclei. However, it should be pointed out that while the relative error on the quadrupole moments between various isotopes should be small, there is an uncertainty of perhaps 20% in the electronic factor needed to extract the spectroscopic quadrupole moment. The magnetic moments are characteristic of the odd nucleon in odd-A nuclei and prove to be useful in identifying the shell model orbitals that are occupied. While a complete discussion is given in Ref. 23, it is pointed out here that the moments of the $9/2^-$ states in Tl are very similar to other spin 9/2 moments in the region of the chart of nuclides and hence supports assignment of the $\pi h_{9/2}$ configuration. Thus, this isomeric state in Tl (Z=81) represents an intruder proton from above the Z = 82 closed shell.

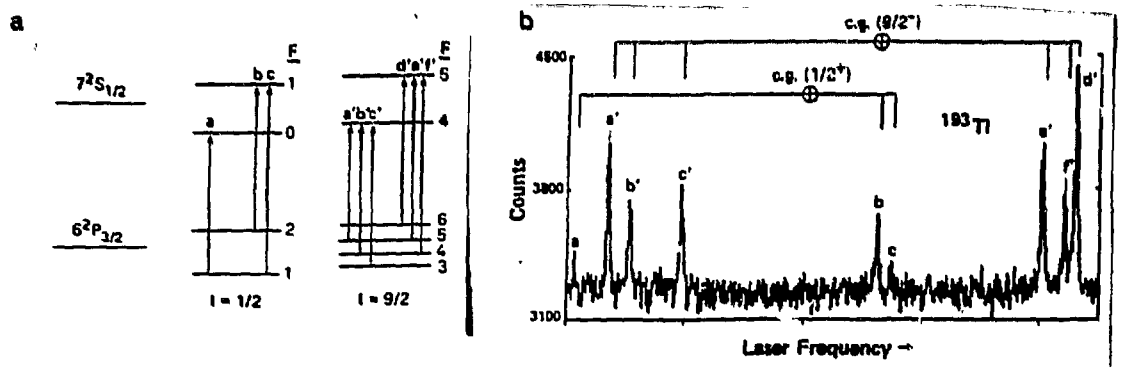

Figure 5. (a) Hyperfine structure for the 6 $^2P_{3/2}$ and 7 $^2S_{1/2}$ atomic states for I = 1/2 and 9/2 nuclei (not to scale). The transitions observed in ^{193}Tl are identified. (b) A sample of the data which displays the hfs from ^{193}Tl^g ($I^\pi = 1/2^+$) and ^{193}Tl^m ($I^\pi = 9/2^-$). The frequency shift between the centers of gravity of the transitions for the two isomers is apparent.

Part of the motivation for this experiment was to determine if the $h_{9/2}$ orbital intrudes into the low excitation energy region of Tl due to the onset of deformation or if other phenomena were involved. The quadrupole moment can be used to obtain a measure of the deformation of the nucleus. It is clear from the band of states built on the $9/2^-$ state that strong coupling holds and for axially symmetric nuclei, the well-known[24] formula

$$Q_s = Q_o \frac{3K^2 - I(I+1)}{(I+1)(2I+3)} \qquad (6)$$

can be used to deduce the intrinsic quadrupole moment. Further, by assuming an axially symmetric ellipsoid, the nuclear deformation β_2 can be deduced from the expression[35]

$$Q_o = \frac{2ZA^{2/3}r_o^2\beta_2(1+0.36\beta_2)}{(5\pi)^{1/2}}. \quad (7)$$

Values of Q_s, Q_o, and β_2 deduced for the light odd-A isotopes in the $9/2^-$ level are given in Table 2. These data seem to support a trend to larger deformation as one goes farther from stability.

Table 2. Quadrupole moments and deformations of light Tl isotopes.

Tl Isomer	Q_s (eb)	Q_o (eb)	β_2 from Q_o	$<\beta_2^2>^{1/2}$ from isomer shift
193g				0.099(1)
193m	-2.20(2)	-4.04(3)	-0.144(1)	0.158(1)
191m	-2.28(3)	-4.18(5)	-0.151(2)	0.170(2)
189m	-2.29(4)	-4.21(7)	-0.153(3)	0.181(2)
187m	-2.43(5)	-4.45(9)	-0.162(4)	

Another indicator of increasing deformation is the shift in the frequency of the 535 nm atomic transition with a change in the nucleus, ie isomer and isotope shifts. The isotope shifts are composed of a normal mass shift of ~ 8 MHs between adjacent masses, the specific mass shift which is small for large A, and the field shift. The field shift can be approximated very well in this region[26,27] by an electronic factor times $\delta < r^2 >$. While the electronic factor is difficult to calculate explicitly, it should be virtually the same for all the Tl isotopes. To deduce the proportionality factor in our analysis we employed the droplet model,[28] which reproduces rms radii throughout the periodic table where deformations are known. One additional assumption that Tl is spherical for a neutron number close to the magic number 126 was made. The electronic factor needed to make the deformations of ^{207}Tl and ^{200}Tl 0 was used to deduce the field shifts of the other isotopes. The resulting field shifts are shown in Fig. 6 in comparison with the predictions of the droplet model with different deformations. The figure indicates that the odd-A Tl $1/2^+$ ground states gradually increase in deformation as the A decreases, reaching a value near 0.1 in ^{193}Tl while the deformation of the $9/2^-$ isomer exceeds 0.15 in ^{193}Tl and increases to 0.18 by ^{189}Tl. The large isomer shift in ^{193}Tl is obvious even in the raw data (see Fig. 5), and is ascribed to quadrupole deformation under the assumption that the monopole radial contribution from the change of single-particle orbit is relatively small, as suggested by spherical shell-model calculations which include the giant monopole resonance.[29] The deformations deduced for the light odd-A Tl isotopes using this technique are also listed in Table 2. Once again the values indicate that the deformation increases as A decreases. The difference in deformations obtained from the spectroscopic quadrupole moments could be accounted for by the 20% error involved in calculation of the electronic factor needed to deduce the spectroscopic

quadrupole moment, but it has also been suggested that the discrepancy can be accounted for by the violation of strong coupling and axial symmetry, which would discredit our method of obtaining β_2 from the spectroscopic quadrupole moments.

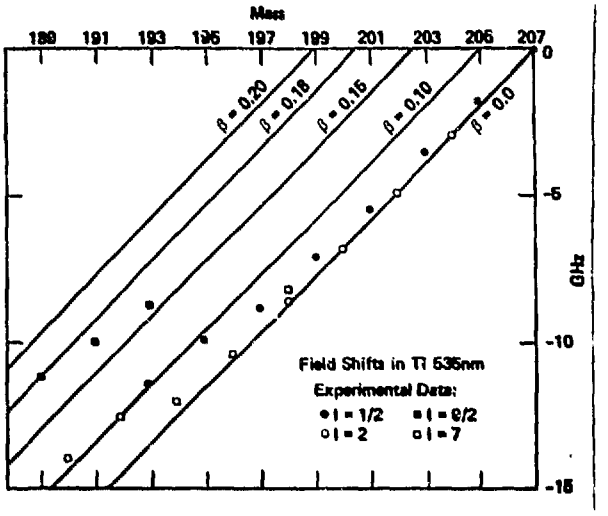

Figure 6. Experimental field shifts in Tl compared to predictions with different droplet-model deformations.

A deformed shell model calculation was made to see if all the features of the intruding $\pi h_{9/2}$ could be explained. While the details of the calculation[22] will not be given here, it predicted the observed drop in the energy of the intruder state near mass 190 and also reproduced the energy of the first excited state in the $9/2^-$ band. This was achieved by an increasing deformation with decreasing A close to the values observed in the UNISOR experiment. The calculation showed that the band structure throughout this region of slowly changing deformation remained constant, primarily because an increase in neutron pairing correlations compensated for the increase in deformation.

6. Future Directions with Laser Techniques

6.1. More Sensitive Detection or Greater Sensitivity

Several experiments are planned to measure magnetic moments, quadrupole moments, and isotope shifts for other species that can be produced in good intensity with the current UNISOR ion sources. For our most recent experiment on the Tl isotopes, it was necessary to achieve a current of 10^5 ions/s in order to detect hyperfine structure resonances over the background produced by the beam and the radioactivity. Without the background, much smaller count rates could be utilized to make the measurements. One way to reduce the background would be to require a coincidence between a beam particle and the de-exciting photon. With the ion source used for Tl separation, this was not possible because of a large component

of stable isotopes or molecules in the beam, thus swamping the particle detector with signals. For elements where the "junk" beams are very small, we will use the coincidence technique to increase the sensitivity.

6.2. Laser Ion Sources

Another possible future development would be the construction of a laser ion source. Feasibility studies[30] have been made of a system which would incorporate a helium gas transport of the activity to a cold finger. Periodically, the sample would be desorbed from the cold finger by a pulsed laser beam and a second laser would be used to ionize the atoms of interest in the resulting vapor cloud. Since the beam would be much purer (essentially no "junk" beams), this would enable the use of the coincidence technique to attain higher sensitivity. Also, because of the pulsing, the beam intensity in a pulse would be much higher than the average intensity thus making the signal to background much higher during the pulse. Thus, by timing the laser spectroscopy with the laser generating the pulses in the ion-source, much higher sensitivity could be achieved.

7. Acknowledgements

Nuclear physics research at the University of Tennessee is supported by Grant No. DE-FG05-87ER40361 with the Department of Energy. UNISOR is a consortium of universities, the State of Tennessee, Oak Ridge National Laboratory and is supported by them and by the U. S. Department of Energy under Contract No. DE-AC05-76OR0033 with Oak Ridge Associated Universities.

8. References

1. E. W. Otten, in *Intl. Conf. on Properties of Nuclei Far From Region of Beta Stability*, (1970), Vol. 1, p. 301.
2. C. Duke, H. Fischer, J.-J. Kluge, H. Kremmling, Th. Kuhl, and E. W. Otten, Phys. Lett. **60A**, 303 (1977).
3. S. L. Kaufman, Opt. Comm. **17**, 309 (1976).
4. Th. Meier, H. Huhnermann, and H. Wagner, Opt. Comm. **20**, 397 (1977).
5. K.-R. Anton, S. L. Kaufman, W. Kelmpt, G. Moruzzi, R. Neugart, E. W. Otten, and B. Schinsler, Phys. Rev. Lett. **40**, 642 (1978).
6. H. K. Carter and C. R. Bingham, in *Future Directions in Studies of Nuclei Far From Stability*, edited by J. H. Hamilton, E. H. Spejewski, C. R. Bingham, and E. F. Zganjar (North Holland, Amsterdam, 1979), p. 83.
7. C. R. Bingham, J. A. Bounds, H. K. Carter, R. L. Mlekodaj, J. C. Griffin, and W. M. Fairbank, Jr., Nucl. Instru. Meth. in Phys. Res. **B26**, 426 (1987).
8. S. Gerstenkorn and P. Luc, *Atlas du Spectre d'Absorption de la Molecule d'Iode*, editions du C.N.R.S. (15 quai Anatole France, 75700, Paris, 1978).
9. H. K. Carter, C. R. Bingham, D. J. Pegg, M. L. Gaillard, E. F. Zganjar, and

P. M. Griffin, Nucl. Instru. and Methods **202**, 361 (1982).
10. H. A. Schuessler, E. C. Benck, F. Buchinger, H. Iimura, Y. F. Li, C. R. Bingham, and H. K. Carter, to be published in *Proceedings of the Intl. Symp. on Lasers in Nuclear Physics*, Riken, Japan, Sept., 1991.
11. M. L. Gaillard, D. J. Pegg, C. R. Bingham, H. K. Carter and R. L. Mlekodaj, Phys. Rev. **A26**, 1975 (1982).
12. H. J. Andrä, in *Beam-Foil Spectroscopy*, edited by I. A. Sellin and D. J. Pegg (Plenum, New York, 1976), Vol. 2, p. 835.
13. D. J. Pegg, M. L. Gaillard, C. R. Bingham, H. K. Carter, and R. L. Mlekodaj, Nucl. Instrum. Methods **202**, 153 (1982).
14. T. Anderson, O.JH. Madsen, and G. Sörensen, Phys. Scr. **6**, 125 (1972).
15. E. Jiménez, J. Campos and D. Sanchez, J. Opt. Soc. Am. **64**, 1009 (1974).
16. K. A. Mohamed, G. C. King and F. J. Read, J. Phys. **B10**, 1835 (1977).
17. R. E. Silverans, G. Borghs, D. De Bisschop, M. Van Hore, and J-M. Van den Cruyce, J. Phys. **B14**, L15 (1981).
18. L. Ward, A. Wännström, A. Arnesen, R. Hallin and O. Vogel, Phys. Scr. **31**, 149 (1985).
19. P. Juncar, C. R. Bingham, J. A. Bounds, D. J. Pegg, H. K. Carter, R. L. Mlekodaj, and J. D. Cole, Phys. Rev. Lett. **54**, 11 (1985).
20. J. E. M. Goldsmith, *et al.*, Phys. Rev. Lett. **41**, 1525 (1978).
21. E. Arnold, *et al.*, Phys. Lett. **90A**, 399 (1982).
22. J. A. Bounds, C. R. Bingham, P. Juncar, H. K. Carter, G. A. Leander, R. L. Mlekodaj, E. H. Spejewski, and W. M. Fairbank, Jr., Phys. Rev. Lett. **55**, 2269 (1985).
23. J. A. Bounds, C. R. Bingham, H. K. Carter, G. A. Leander, R. L. Mlekodaj, E. H. Spejewski, and W. M. Fairbank, Jr., Phys. Rev. **36**, 2560 (1987).
24. A. Bohr and B. R. Mottelson, *Nuclear Structure* (Benjamin, London, 1975), Vol. 2.
25. K. E. G. Löbner, M. Vetter, and V. Hönig, Nucl. Data Tables **A7**, 495 (1970).
26. R. C. Thompson, *et al.*, J. Phys. **G9**, 443 (1983).
27. J. Bonn, *et al.*,Z. Phys. **A276**, 203 (1976).
28. W. D. Meyers and K. H. Schmidt, Nucl. Phys. **A410**, 61 (1983).
29. J. Speth, L. Zamick, and P. Ring, Nucl. Phys. **A232**, 1 (1974).
30. W. M. Fairbank, Jr. and H. K. Carter, private communication.